

# A MULTI-TRANSITION SEARCH FOR CLASS I METHANOL MASERS

Cara Denise Battersby

MIT Haystack Observatory REU  
Summer 2004

Mentors: Preethi Pratap and Phil Shute

## ABSTRACT

Class I methanol masers have been detected in star forming regions, and may be a critical link in detecting very early star formation. Class I methanol masers are pumped by collisional excitation followed by spontaneous radiative decay and often occur in the outflows of young stars. We have used the Haystack 37m antenna to conduct a search for Class I methanol masers at three transitions towards the known star-forming regions of s255, s235, omc2, and w75 north and west. We detected masers and mapped the surrounding region. Methanol masers that are coincident in position and velocity between 36 GHz and 44 GHz have been found, as well as emission at 44 GHz with no corresponding emission at 36 or 25 GHz. There have been no detections at 25 GHz. A comparison of line widths is also presented. The hope is that these data will facilitate modeling of the pumping mechanism of these masers and the surrounding physical environment.

## I. INTRODUCTION

Haystack Observatory is conducting an ongoing search for class I methanol masers. Methanol masers are classified based on their pumping mechanism, masing transition, and loosely with their proximity to other astronomical objects. Class II methanol masers have been fairly well studied and their radiative pumping mechanism is more clearly understood. Class I methanol masers, however, are generally offset from centers of star formation, compact H II

regions, and strong infrared sources, and thus, are commonly overlooked. The aim of the search is to gather more information about these class I masers in order to better understand how they work and what their presence can tell us about the surrounding region.

Undergraduate researchers have been thoroughly involved in this project. Before I came here this summer, masers had been detected at the sources I've inspected at 44 GHz, and in some cases they had also been found at 36 GHz.

However, with many different undergraduates working with this project in the past, the data was somewhat erratic and incomplete. I've made former observations more consistent and taken new observations to fill in the missing data. I've also extended the search to the 36 and 25 GHz transitions for all the sources. There have been several extensive surveys for methanol masers at the 44 GHz transitions, but very few multi-transition searches. The additional data at these new transitions are important for the modeling and understanding of the pumping mechanism.

## **II. OBSERVATIONS AND DATA REDUCTION**

Observations were made in June and July 2004 with the NEROC Haystack Observatory 37m antenna near Westford, MA. Data was taken on days (and nights) of relatively good weather. Typical system temperatures at 25 GHz were between 110 and 130K. At 36 and 44 GHz the typical system temperatures ranged from 190 and 280K. We used an integration time of five minutes for each point, though for many points, observations were repeated resulting in much higher integration times. At 44.069488 GHz and 36.169240 GHz measurements were made using beam switching spectroscopy, while measurements made at 24.933468 GHz used frequency switching. At 25 and 36 GHz we used one video converter which corresponds to a spectral resolution of 5.2 kHz and at 44 GHz we used two video converters for a spectral resolution of 10.5 kHz. We used a bandwidth of 17.8 MHz for maser searching and 160 MHz for planet pointing. Pointing

measurements were performed roughly every hour and a half.

Data was downloaded using umbrella and saved in CLASS (Continuum and Line Analysis Single-dish Software). Baselines were removed in CLASS. The multiple integration sums of a single point were weighted by noise, not time, in order to achieve the best signal to noise ratios. Spectral maps and line comparisons were achieved with CLASS, while the contour maps were made using GreG (Grenoble Graphic).

Planet pointing was performed at least once every observation day. This allows us to compare the known flux of a planet (typically Venus or Jupiter) with the degrees of intensity that we receive, saying for example, that every degree corresponds to 10 Janskys. Correcting for the variable aperture efficiency enables us to give an accurate estimation for the flux of our peak intensities. Due to the fact that many observations were repeated more than once on different days, we have just taken an average flux to degree ratio and error accordingly to apply a flux to our intensities, assuming that the aperture efficiency is not largely variable. There is still an additional error imposed upon our data due to the changing aperture efficiency. Line widths, peak intensities, position, and their errors were determined by fitting gaussian curves in CLASS.

## **III. INTRODUCTION TO THE SOURCES**

The molecular cloud s235 contains two regions, one that surrounds the s235 H II region. The second region, the one we are studying, is a hot, dense area of

active star formation. It is 3-4 solar masses and approximately  $2\text{-}5 \times 10^5 \text{ cm}^{-3}$  in density (Evans 1980).

S255 is a molecular cloud that is associated with a group of H II regions, but is otherwise isolated. The cloud exhibits distinguishing characteristics of star formation, including maser activity (Richardson 1985).

OMC-2 is a young cluster in the early stages of vigorous star formation only 450 pc away (Peterson 2001). OMC-2 seems to be an intermediate evolutionary stage between the nearby molecular clouds, OMC-1 and OMC-3. The core has a high density and a temperature of about 24K. The OMC-2 molecular cloud is 12 arc minutes north of the trapezium OB star cluster (Castets 1995).

The W75 molecular cloud is a star forming region about 2 kpc away. It is part of the larger complex of dense molecular clouds, Cygnus X. I have looked at parts of w75 north and west,

and another undergraduate has been studying w75 south.

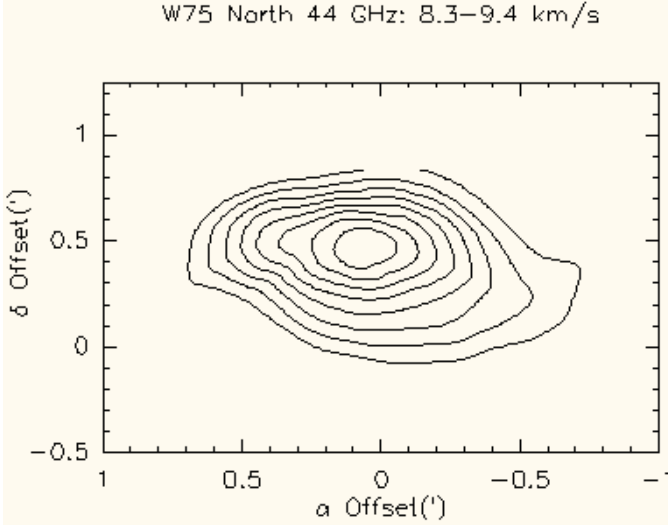
## IV. RESULTS

Table 1 summarizes the detections that we've made. Masers had already been detected at 44 GHz in our chosen sources, but we did not know what to expect at the 36 and 25 GHz transitions. For the sources that we've claimed have no detection, it is important to realize that there was simply no detection at the noise level to which we looked. Finding any kind of signal that is smaller than an rms of 2 Janskys could be very time-consuming, and would probably not be the best way to use your precious time on the Haystack antenna. Also, some of the detections at 36 GHz do not have a large signal to noise ratio, and in order to learn more about those masers, a great deal more integration time would be necessary. As I stated previously, though, that was not the best use of our time on the telescope.

TABLE 1  
Detection Summary

Source	Center Position	44.069488 GHz	36.169240 GHz	24.933468 GHz
	$\alpha_{1950}$ (h m s) (+ -) $\delta_{1950}$ ( $^{\circ}$ ` ``) $V_{\text{LSR}}$	Detection? Flux (Jy)*	Detection? Flux (Jy)*	Detection? Flux (Jy)*
W75 west	20:36:45.1 +42:26:01 10.2	Yes 28 +/- 3	Yes 27 +/- 6	No 2
W75 north	20:36:50.5 +42:27:01 8.9	Yes 65 +/- 5	No 5	No 2
S235B	05:37:32 +35:40:50 -16.1	Yes 14 +/- 4	Yes 4	No 2
S255	06:10:01 +18:00:44 11.5	Yes 242 +/- 4	No 5	No 4
OMC-2	05:32:59.8 -05:11:29 11.6	Yes 238 +/- 4	Yes 4	No 2

\* When there has been a detection, the flux refers to the peak intensity and it's error. When there has not been a detection, the flux refers to the rms noise to which we looked for a signal.



**Figure 1:** Contour map of w75 north at 44 GHz. The contours are of flux beginning at 5.6 Jy and going up in increments of 2.8 Jy. The offsets are in arc minutes with the central position as stated in table 1.

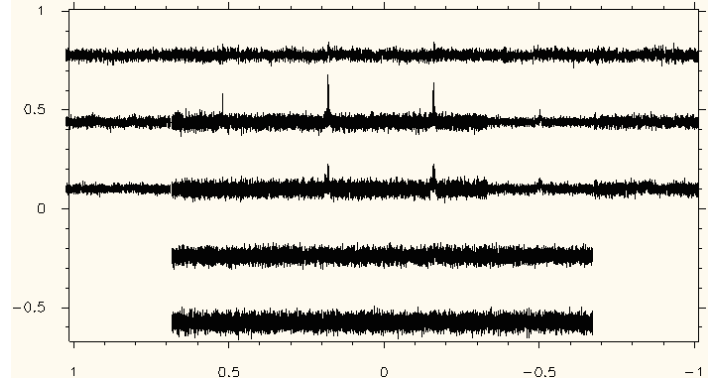


**Figure 2:** Map of the line spectra of w75 north at 44 GHz. The x-axis of each spectra is measured in km/s while the y-axis is the flux. The offsets are as in figure 1.

#### IV. i. W75 north

W75 north at 44 GHz exhibits strong emission that is relatively compact. See the peaks for w75 north in Figure 13. The best gaussian fit was achieved with two curves, though it is not otherwise clear that there is any sort of double peak structure. The position of the first peak is  $8.38 \pm 0.13$  km/s and the second peak is  $8.87 \pm 0.01$  km/s. The center of the peak structures is approximately 8.9 km/s. The line width of the first peak is  $4.03 \pm 0.28$  and of the second peak  $0.28 \pm 0.01$ . The intensity of the first peak is  $14.5 \pm 5.1$  Jy. The intensity of the second peak is  $64.9 \pm 5.1$  Jy, making it the much stronger peak, and due also to the line width, the main maser feature, while the second peak could be due to thermal emission. Figure 2 is a map of the line spectra, with the offsets in arc minutes from the central peak noted in table 1. Figure 1 is a contour map of w75north at 44 GHz where the contours are of flux. The contour map is intended to clarify the

structure of the maser and exhibit how the intensity of emission drops off.

W75 north at 36 GHz shows only thermal emission. There is no narrow peak, only wideband emission. The map, however, does extend down into w75 west where there is maser activity as shown in Figures 3 and 4. Figure 4 is a map of the line spectra and Figure 3 is a contour map of the flux. The contour map shows the emission at w75 north and at w75west where it is quite the opposite. The contours increase sharply until it reaches a high, and clear peak. Since class I methanol masers are pumped by collisional excitation followed by spontaneous radiative decay, there is some thermal activity, thus the thermal emission at 36 GHz. The masers found are commonly a tall, narrow peak superposed over thermal emission. The emission found at 36 GHz is the same, but without the peak that makes it a maser.

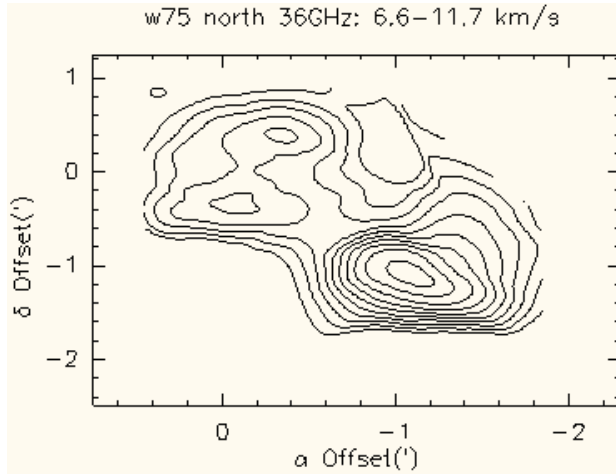


**Figure 3:** Contour map of w75 north at 36 GHz. The emission in the upper left is just thermal emission whereas the emission in the lower right extends into the maser in w75west. The contours are of flux and begin at 7.7 Jy and move up in increments of 2.6 Jy. The offsets are as in figure 1.

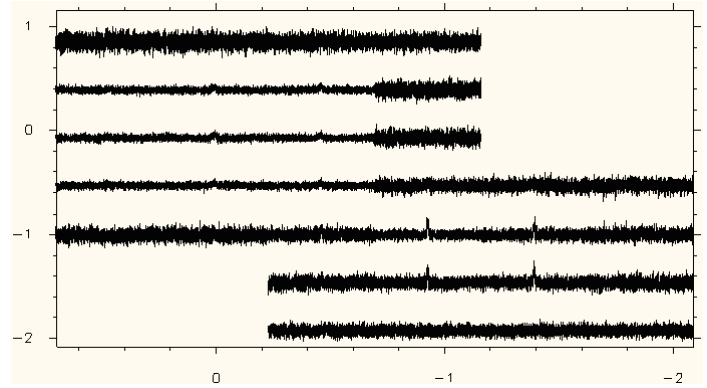


**Figure 4:** Map of the line spectra of w75 north at 36 GHz as it transitions into w75west. W75 west is located in the lower right and contains the maser, and w75 north is the thermal emission in the upper left. The offsets are as in figure 1.

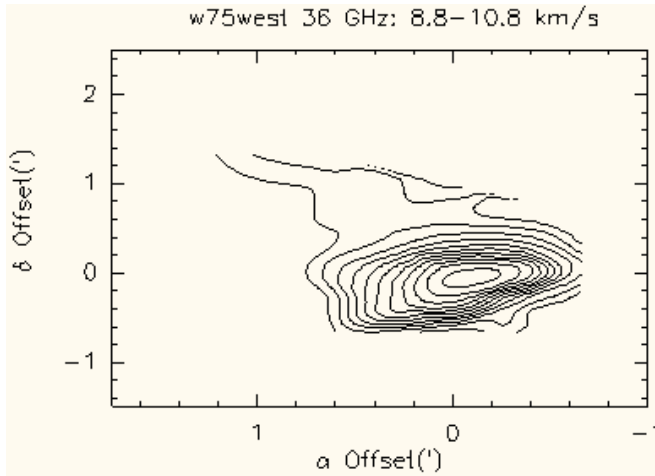


**Figure 5:** w75 west contour map at 36 GHz focused in the velocity range of the maser. The contours being at 7.7 Jy and increase in increments of 2.6 Jy. The offsets are in arc minutes from the center position given in table 1.

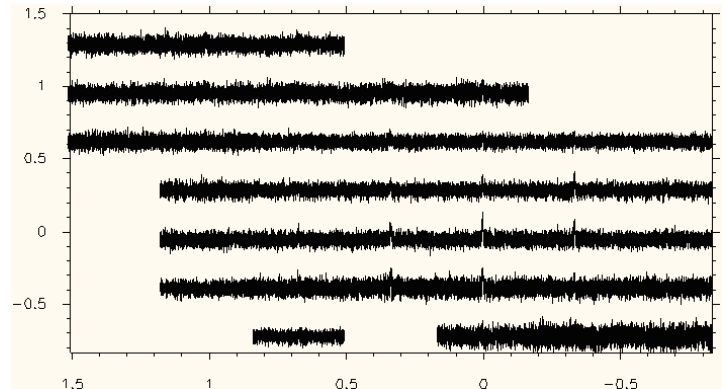


**Figure 6:** map of the line spectra for w75 west at 36 GHz. Note that the thermal emission is not seen in this map, as it is in the w75 north map because there is more noise. The offsets are as in figure 5.

#### IV. ii. W75 west

At 36 GHz w75 west exhibits maser emission. The gaussian fit is best done using 5 curves, though there only seem to be 3 peaks. One curve is used to

represent the thermal emission over which the maser peak is superposed. The first peak of interest occurs at  $9.46 \pm 0.18$  km/s with a line width of  $0.67 \pm 0.28$  and an intensity of  $13.5 \pm 0.4$

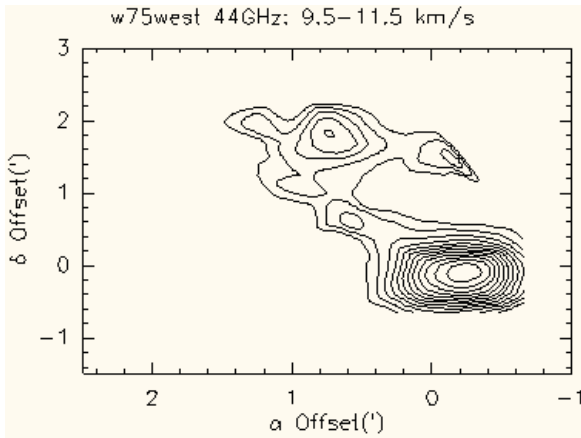


**Figure 7:** Contour map of w75west at 44 GHz. The velocity range is focused on the central velocity at w75 west, and not the velocity of w75 north, thus the larger looking peak for west even though north is actually stronger. The contours begin at 5.6 Jy and increase in increments of 2.8 Jy.

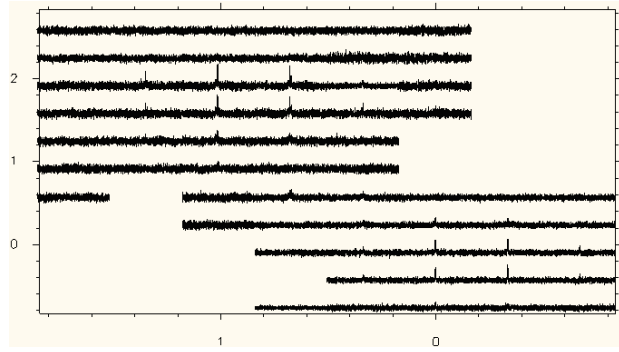


**Figure 8:** Line spectra map of w75 west at 44 GHz. W75 west is located in the lower right and w75 north is in the upper left. The offsets are in arc minutes relative to the central position given in table 1.

Jy. The second and largest peak of interest is at  $9.86 \pm 0.02$  km/s with a line width of  $0.26 \pm 0.06$  and an intensity of  $26.7 \pm 0.4$  Jy. The final peak is located at  $10.28 \pm 0.03$  km/s with a line width of  $0.43 \pm 0.08$  and an intensity of  $20.3 \pm 0.4$  Jy. The line spectra map, Figure 6, continues into the w75 north region, but we don't detect the thermal emission because the noise is too large in comparison with the w75 north map.

At 44 GHz the maser emission is similar. See the peaks for w75 west in Figure 14. There is a multiple peak structure that is more evident at 44 GHz. The 44 GHz peak is best fit with 3 gaussian curves, one for the thermal emission and then the other two for the double peak. The first peak is at  $10.18 \pm 0.01$  km/s with a line width of  $0.72 \pm 0.02$  and an intensity of  $28.4 \pm 3.0$  Jy. The second peak is at  $10.90 \pm 0.01$

with a line width of  $0.27 \pm 0.01$  and an intensity of  $23.8 \pm 3.0$  Jy.

What is interesting about w75 west is that the emission at 36 GHz is stronger than the emission at 44 GHz as shown in Figure 9. This is very peculiar and interesting. From papers on the CO outflows in w75 (Davis et. al 1997, Fischer et. al 1984) it seems as though both w75 north and west are somewhat in this outflow. There is also a velocity shift from w75 north to west at 44 GHz as shown in figure 10. The velocity shift indicates that perhaps one of w75 north or west is in the outflow. If it is w75west that is in the outflow, and that is the one source for which 36 GHz emission is stronger than 44 GHz emission, then we can make a conclusion that the outflow causes the 36 GHz emission to be stronger. This is a hypothesis that we plan to further investigate and test.

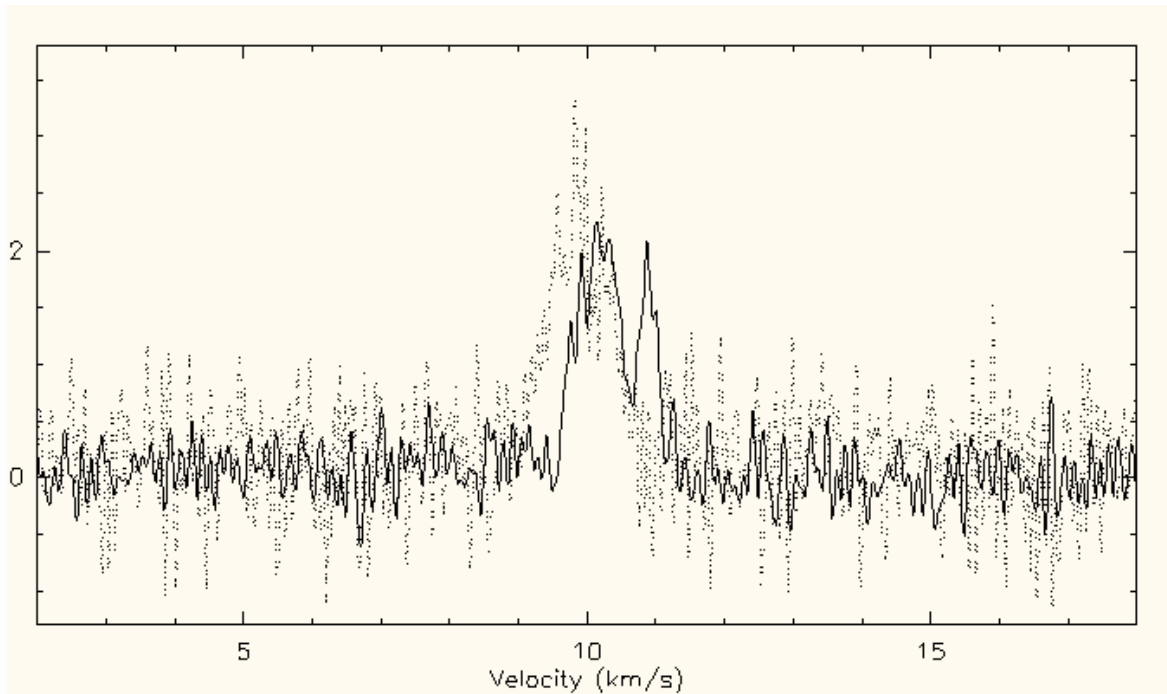


**Figure 9:** line spectra of w75 west at the central position. The dotted line is 36 GHz and the solid line is 44 GHz.

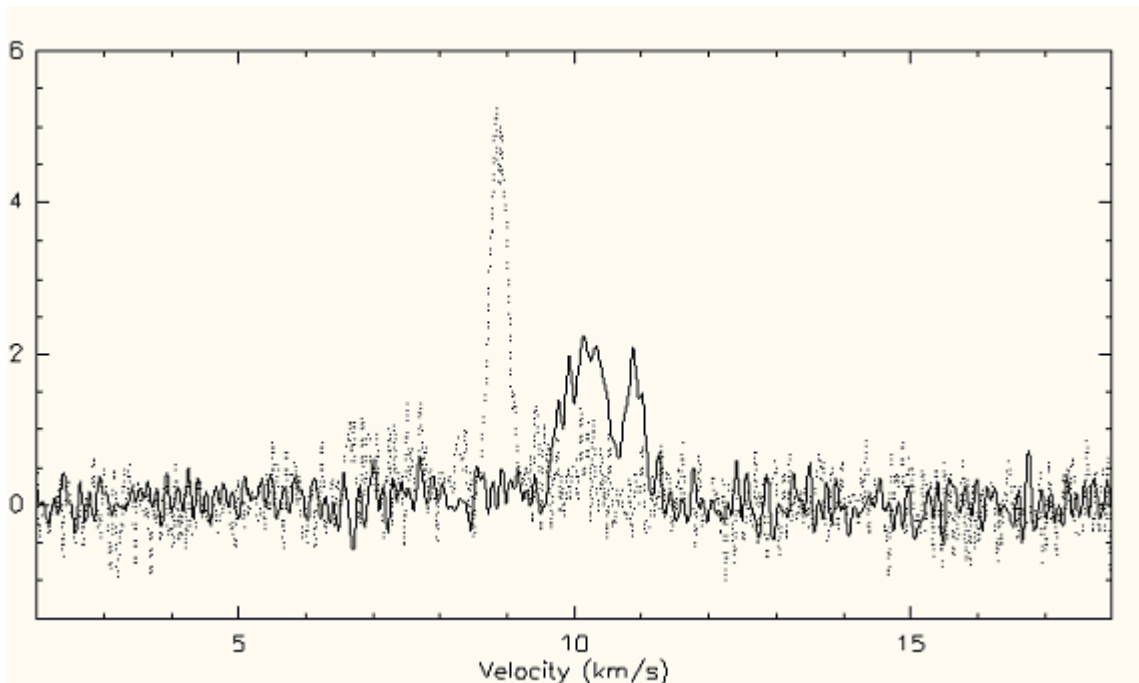


**Figure 10:** line spectra of w75west and north at 44 GHz at their peak position (w75west: offset (0,0), w75north: offset (0.169, 0.504)). Note the velocity shift.

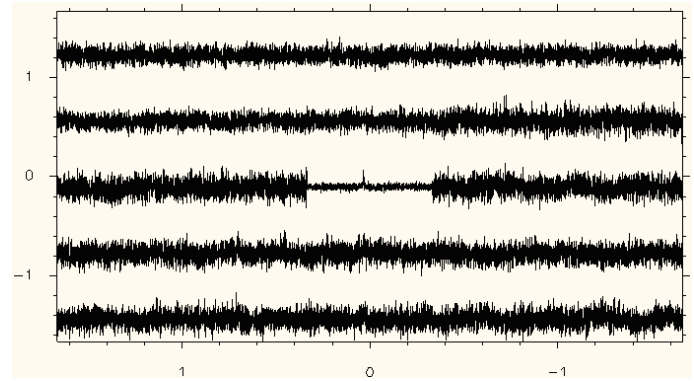
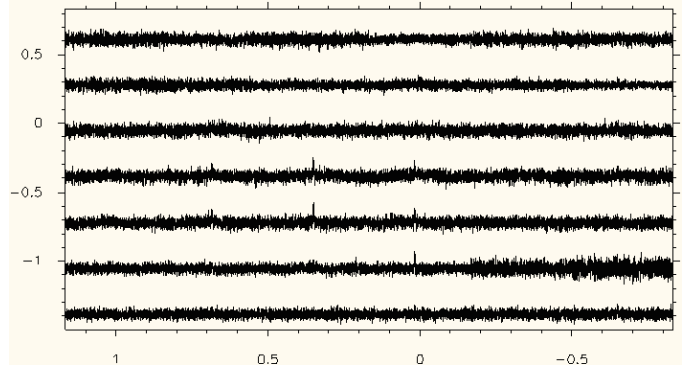
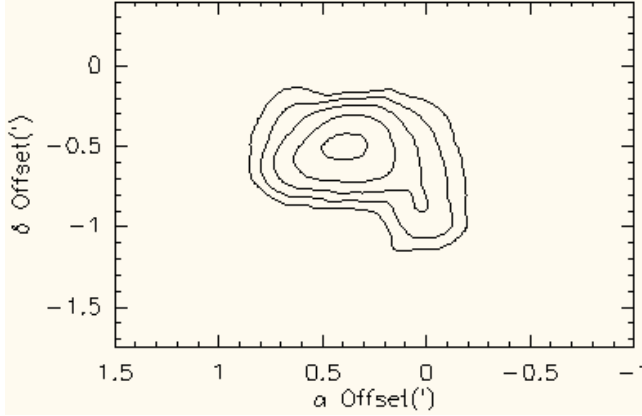


**Figure 11:** top left: S235B at 44 GHz. The contours begin at 8.4 Jy and increase in increments of 2.8 Jy. Top right: line spectra map of S235B at 44 GHz. Note that the maser activity is offset from center. Bottom right: line spectra map of S235B at 36 GHz. All offsets are in arc minutes relative to the central position given in table 1.

#### IV. iii. S235B

The 44 GHz peak in S235B is relatively weaker than the other 44 GHz peaks. The position of the maser is also offset from our central position by less than an arc minute. We fit the peak using two gaussians. The first peak was at  $-16.08 \pm 0.02$  km/s with a line width of  $0.23 \pm 0.04$  and an intensity of  $14.4 \pm 4.1$  Jy. The second peak is at  $15.93 \pm 0.03$  with a width of  $0.99 \pm 0.09$  and an intensity of  $14.1 \pm 4.1$  Jy. The second peak is just a wing on the first peak. Figure 11 shows the spectra, the slightly wider right side than left side is caused by the wing. See the peaks for S235B at Figure 12.

Many integrations were taken by a student who came before me at 36 GHz at the center position. These many integrations led to a signal detection, though very small. A gaussian was not

fitted to this peak, especially because the signal is smaller than the surrounding noise, and little could be gained. However, s235b may be part of an outflow, in which case we will perform more integrations at the appropriate offset in order to test our hypothesis at 36 GHz.

#### IV. iv. S255

S255 shows an interesting double peak structure at 44 GHz. Figure 16 shows this structure and Figure 17 shows contour maps of the peaks. Figure 17, top left, shows the shorter peak while Figure 17, top right, shows the second, larger peak. I used two gaussians to fit the peaks. The first, smaller peak is located at  $10.59 \pm 0.01$  km/s with a line width of  $0.49 \pm 0.01$  and an intensity of  $75.4 \pm 4.3$  Jy. The second, larger peak is located at  $11.54 \pm 0.01$

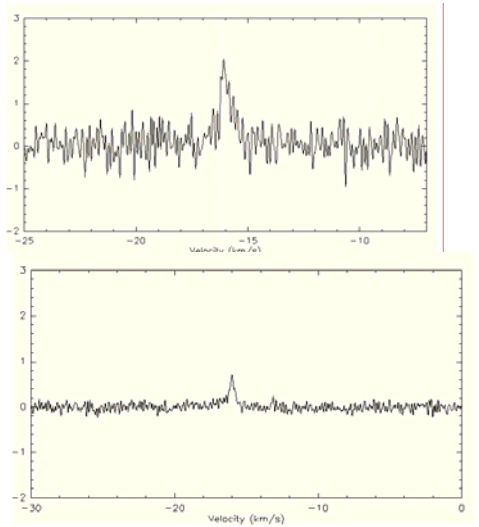


**Figure 12:** S235B. Top is at 44 GHz and at the offset (.33, -.66) arc minutes relative to the center. Bottom is 36 GHz at the center position.

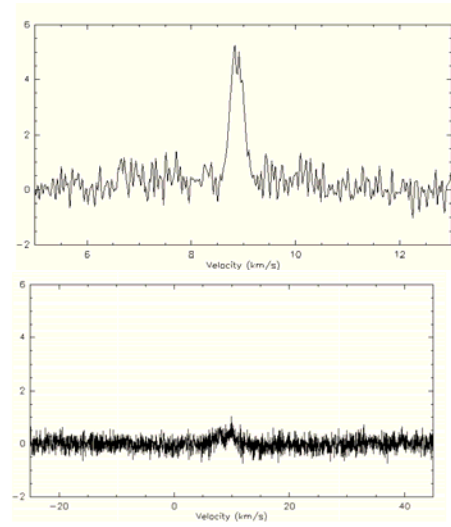


**Figure 13:** W75 north. Top is at 44 GHz at the offset (0.169, 0.504) arc minutes relative to the center. Bottom is 36 GHz at the center position.

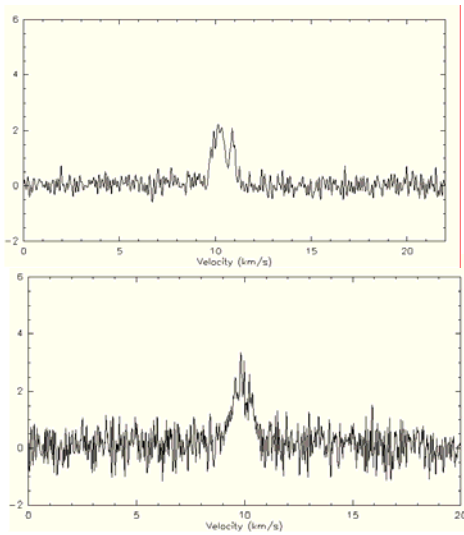


**Figure 14:** W75 west. Top is at 44 GHz at the center position. Bottom is at 36 GHz, also at the center position.

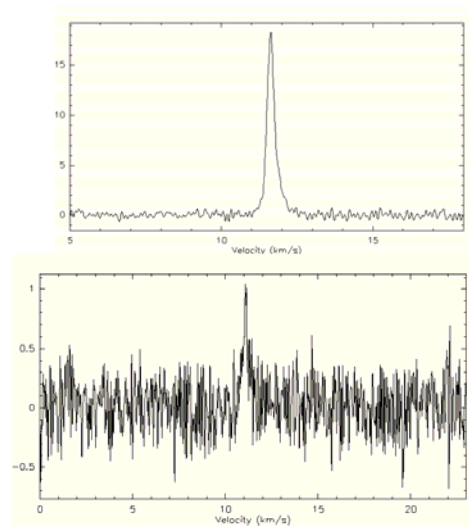


**Figure 15:** OMC-2. Top is at 44 GHz, center position. Bottom is at 36 GHz, center position.

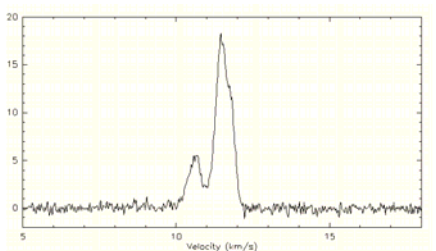


**Figure 16:** S255. Double peak structure at 44 GHz, offset from center by (-0.733, 0.367) arc minutes.

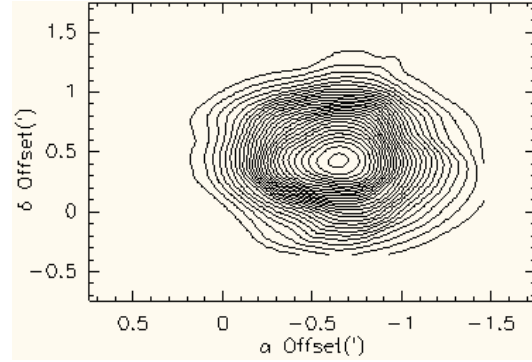
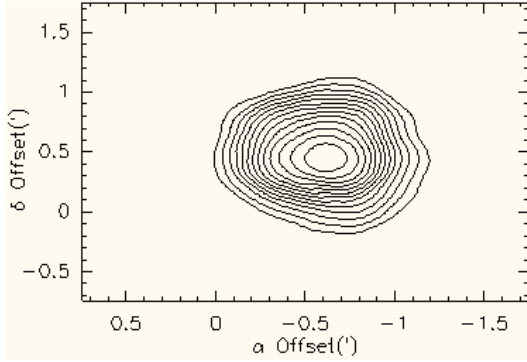
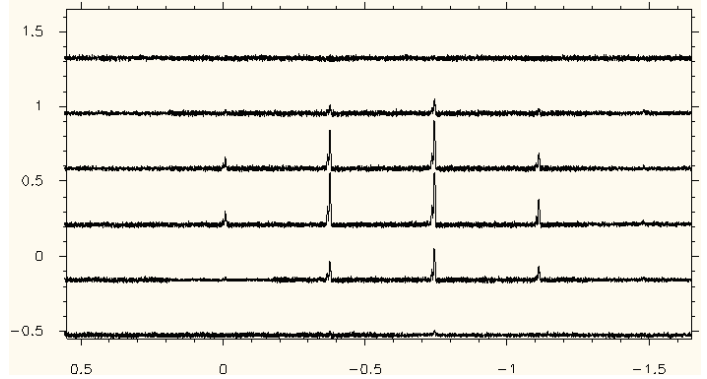


**Figure 17:** Top left: S255 at 44 GHz from 9.9-11.0 km/s. The contours begin at 8.4 Jy and increase in increments of 7.0 Jy for both contour maps. Top right: S255 at 44 GHz from 11.0-12.2 km/s. Bottom right: line spectra map of S255 at 44 GHz. All offsets are in arc minutes and relative to the central peak given in table 1.



km/s with a line width of  $0.59 \pm 0.01$  and an intensity of  $242.2 \pm 4.3$  Jy, the largest we've found. The double peak structure is caused by maser components moving at slightly different velocities. However the two peaks are coincident in position. There was no detection at 36 GHz at the noise level to which we searched.

#### IV. v. OMC-2

Maser emission was detected in the molecular cloud OMC-2 at 44 GHz. The peak is the second strongest that we've found. It is best fit using 3 lines, one for thermal emission, the peak, and a little wing on the right side. The position of the peak is  $11.62 \pm 0.01$  km/s with a line width of  $0.25 \pm 0.01$  with an intensity of  $213.0 \pm 3.7$  Jy. It is important to notice that on all these line spectra maps, the scales are not quite the same. OMC-2 at 44 GHz looks as though there is very little noise, but it

has just about as much noise as OMC-2 at 36 GHz, but a much better signal to noise ratio.

The emission detected at 36 GHz is promising but we can't clearly determine anything yet. A gaussian was not fit because the peak is so small, and the noise still mostly dominates its structure. This transition could benefit from more integration time, although the immediacy or necessity of that is not clear at the moment.

At 44 GHz, a map had already been made, but there were only a couple noticeable features. We zoomed in on that area in order to make a more detailed map. When doing this, we noticed that there was a velocity shift between the old data and the new data. The old data at the center position had been integrated many times. While I personally didn't take the data, and thus,

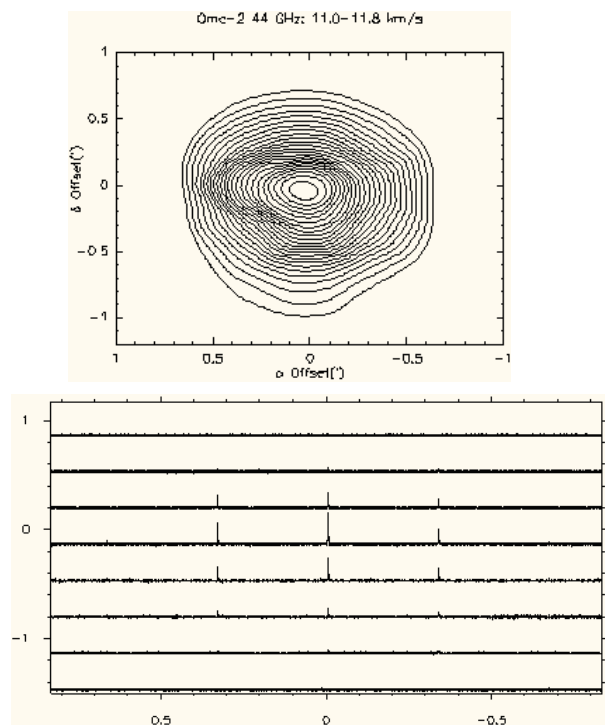


**Figure 18:** Top: Contour map of OMC-2 at 44 GHz. The contours begin at 8.4 Jy and increase in increments of 2.8 Jy. Bottom: Line spectra map of OMC-2 at 44 GHz. All the offsets are in arc minutes with respect to the central position given in table 1.

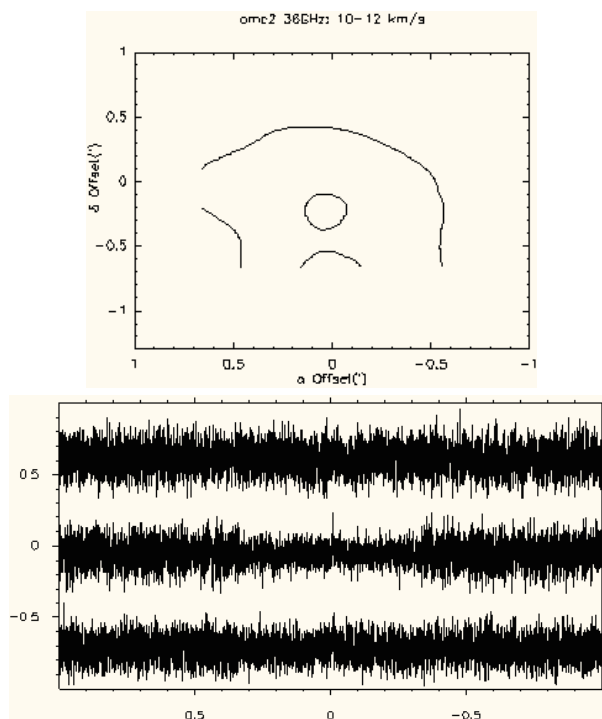


**Figure 19:** Top: Contour map of OMC-2 at 36 GHz. The contours begin at 2.6 Jy and increase in increments of 2.6 Jy. Bottom: Line spectra map of OMC-2 at 36 GHz. All the offsets are in arc minutes with respect to the central position given in table 1.

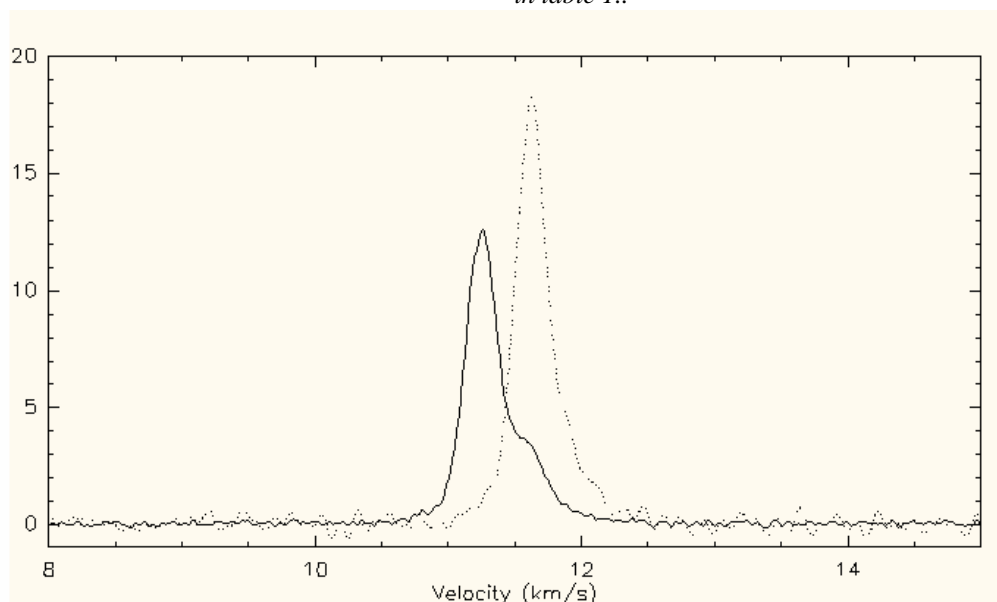


**Figure 20:** OMC-2 at 44 GHz at the central position. The solid line is the older version while the dashed line is the version taken this summer. Notice how the solid wing coincides with the new peak.

can't be sure of its accuracy, we did not detect this kind of shift in any of our other sources with time. One could suppose that if it was a change in instrumentation that it would affect all the sources. There is no simple error that a person taking data could perform in order to cause this velocity shift. So, even though we need to further investigate whether this is an actual shift with time, it is quite an interesting possibility. Notice also how the older version has a wing on the right side, and that wing is coincident with the new-found peak position.

#### IV. vi. Note on 25 GHz

We have not detected any masers at 25 GHz. While more integrations may show some emission, the point is that to the noise level that we detected masers at 44 GHz and 36 GHz, none have been detected at 25 GHz. Whether this simply means that 25 GHz methanol masers are uncommon in the types of sources we looked at or whether it means that they do not exist in the types of sources we've looked at is still unclear. However, this has excited anticipation, and if we do find emission at 25 GHz, we'll know that it's something special.

## V. CONCLUSIONS

We have found some very interesting features and detected and

mapped maser regions. 25 GHz methanol masers are uncommon, or we are unlucky, or they simply do not occur in the type of sources we've looked at. We have a new hypothesis that 36 GHz methanol masers occur most strongly in outflows. There is the possibility that we have detected a time variability in OMC-2 at 44 GHz, which would be quite exciting. I plan to continue researching these possibilities along with new sources under the guidance of Dr. Preethi Pratap. The culminating result of all of this will be a scientific paper concluding all the work done with class I methanol masers.

## REFERENCES

- Castets, A., Langer, W.D. 1995. *Astronomy and Astrophysics*. **294**: 835-854.
- Davis, C.J., Moriarty-Schieven, G., Eisloffel, J., Hoare, M.G., Ray, T.P. 1998. *The Astronomical Journal*. **115**: 1118-1134.
- Evans, N., Blair, G. 1981. *The Astrophysical Journal*. **246**: 394-408.
- Fischer, J., Saners, D.B., Simon, M., Solomon, P.M. 1985. *The Astrophysical Journal*. **293**: 508-521.
- Richardson, K.J., White, G., Gee, G., Griffin, M.J., Cunningham, C.T., Ade, P.A.R. 1985. *Royal Astronomical Society*. **216**: 713-733.

